Chapter 26
Modeling of Large-Strain Cyclic Plasticity Including Description of Anisotropy Evolution for Sheet Metals

Fusahito Yoshida, Takeshi Uemori and Hiroshi Hamasaki

Abstract The present paper describes a framework for the constitutive modeling of a large-strain cyclic plasticity to describe the evolution of anisotropy and the Bauschinger effect of sheet metals that is based on the Yoshida-Uemori kinematic hardening model. In the model, the shapes of the yield and the bounding surfaces are assumed to change simultaneously with increasing plastic strain. An anisotropic yield function that varies continuously with the plastic strain is defined by a non-linear interpolation function of the effective plastic strain using a limited number of yield functions determined at a few discrete points of plastic strain. With this modeling framework, any type of yield function can be used and the convexity of the yield surface is always guaranteed. A set of kinematic parameters can be identified experimentally independent of the anisotropic parameters.

Keywords Constitutive model · Yoshida-Uemori model · Cyclic plasticity · Anisotropy evolution · Sheet metal

26.1 Introduction

The use of constitutive models that properly describe the elastic-plastic deformation behavior is essential for accurate numerical simulation of sheet metal forming. The anisotropy of sheets is of great concern to the forming industry because it strongly

F. Yoshida (✉) · H. Hamasaki
Department of Mechanical Science and Engineering, Hiroshima University,
1-4-1, Kagamiyama, Higashi-hiroshima 739-8527, Japan
e-mail: fyoshida@hiroshima-u.ac.jp

H. Hamasaki
e-mail: hamahiro@hiroshima-u.ac.jp

T. Uemori
Graduate School of Natural Science and Technology, Okayama University,
1-1-1, Tsushima-naka, Kita-ku, Okayama 700-0082, Japan
e-mail: uemori@okayama-u.ac.jp

H. Altenbach et al. (eds.), *From Creep Damage Mechanics to Homogenization Methods*, Advanced Structured Materials 64,
DOI 10.1007/978-3-319-19440-0_26

influences the formability of sheets. Thus, many types of anisotropic yield functions have been proposed in the past, e.g., Hill (1948, 1979, 1990); Gotoh (1977); Barlat and Lian (1989); Barlat et al. (1991, 2003, 2005); Cazacu and Barlat (2001, 2003, 2004); Karafillis and Boyce (1993); Bron and Besson (2004); Banabic et al. (2005); Hu (2005, 2007); Leacock (2006); Vegter and Boogaard (2006); Comsa and Banabic (2008); Steglich et al. (2011); Desmorat and Marull (2011), etc.

Another important issue in material modeling is describing cyclic plasticity behavior. Descriptions of the Bauschinger effect and workhardening have been intensively investigated within the framework of a combined isotropic-kinematic hardening model for the past few decades, e.g., Armstrong and Frederick (1966); Mróz (1967); Krieg (1975); Dafalias and Popov (1976); Ohno (1982); Chaboche and Rousselier (1983); Ohno and Wang (1993); MacDowell (1995); Geng and Wagoner (2002); Yoshida (2000); Yoshida et al. (2002, 2013, 2015); Yoshida and Uemori (2002, 2003); Haddadi et al. (2006); Taleb (2013); for more details, refer to reviews by Chaboche (2008); Ohno (2015). Before 2000, most cyclic plasticity models were constructed within the theory of infinitesimal deformation without considering material anisotropy because they were applied mainly to structural analyses for predicting low-cycle fatigue life and ratcheting. In the early 2000s, some researchers pointed out that the Bauschinger effect of materials greatly affects springback behavior, especially for high-strength steel (HSS) sheets, and several cyclic plasticity models were proposed for springback simulation, e.g., Yoshida and Uemori (2002, 2003); Geng and Wagoner (2002). The present authors previously proposed a model of large-strain cyclic plasticity, so-called 'Yoshida-Uemori (Y-U) model' (Yoshida et al. 2002; Yoshida and Uemori 2002, 2003) to describe the following cyclic plasticity behaviors (see Fig. 26.1) together with the anisotropy of materials:

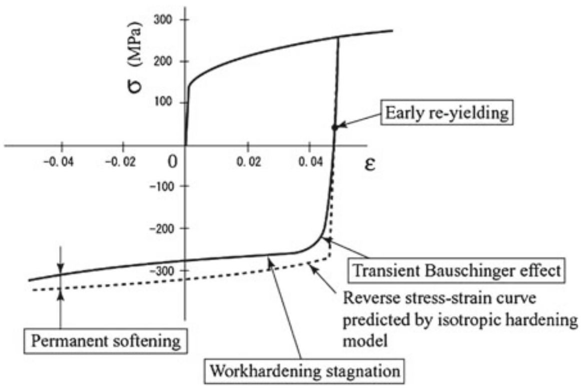

Fig. 26.1 Elastic-plastic behavior in a reverse deformation: early re-yielding, transient Bauschinger effect, workhardening stagnation and permanent softening (Yoshida and Uemori 2003)

- Two stages of the Bauschinger effect: (i) *the transient Bauschinger deformation* characterized by early re-yielding and smooth elastic-plastic transition with a rapid change in the workhardening rate; and (ii) *the permanent softening* observed in a region after the transient period;
- *Workhardening stagnation*, which appears at a certain range of reverse deformation;
- The strain-range and mean-strain dependency of cyclic hardening, i.e., the larger cyclic strain range induces the larger saturated stress amplitudes.

A recent topic of plasticity for sheet metals has been the modeling of anisotropic hardening. Conventional plasticity models assume that the shape of the yield surface does not change during a plastic deformation; consequently, the r-values and flow stress directionality calculated with these models remain constant throughout the deformation. However, some metallic sheets exhibit significant changes in r-value anisotropy and flow stress directionality (e.g., Hu 2007; Stoughton and Yoon 2009; An et al. 2013; Safaei et al. 2014) and the shape of the yield surface (e.g., Tozawa 1978; Kuwabara et al. 1998; Yanaga et al. 2014; Yoon et al. 2014) as plastic strain increases. Although there are some models of the anisotropic hardening (e.g., Hu 2007; Plunkett et al. 2008; Stoughton and Yoon 2009; An et al. 2013; Safaei et al. 2014; Yanaga et al. 2014; Yoon et al. 2014), most of them exclude a description of the Bauschinger effect. Distortion yield function modeling is another type of formulation used to represent the Bauschinger effect and stress-strain responses under non-proportional cyclic loading (e.g., Shiratori et al. 1979; Voyiadjis and Foroozesh 1990; Kurtyka and Życzkowski 1996; Francois 2001; Feigenbaum and Dafalias 2007; Barlat et al. 2011, 2013, 2014). However, to the best of the present authors' knowledge, only Barlat et al.'s homogeneous anisotropic hardening (HAH) model (Barlat et al. 2011, 2013, 2014) reproduces the Bauschinger effect well together with the anisotropy evolution of sheet metals.

The present paper proposes a model of large-strain cyclic plasticity that describes the evolution of anisotropy and the Bauschinger effect of sheet metals based on the Y-U kinematic hardening model. This modeling framework has great advantages over other models. It allows any type of yield function to be used, and the convexity of the yield surface is always guaranteed. A set of kinematic parameters can be identified from experimentally independent of anisotropic parameters.

26.2 Framework of Combined Anisotropic-Kinematic Hardening Model

With the assumption of small elastic and large plastic deformation, the rate of deformation $\boldsymbol{D}$ is decomposed into its elastic and plastic parts, $\boldsymbol{D}^{\mathrm{e}}$ and $\boldsymbol{D}^{\mathrm{p}}$, respectively, as follows:

$$\boldsymbol{D} = \boldsymbol{D}^{\mathrm{e}} + \boldsymbol{D}^{\mathrm{p}} \tag{26.1}$$

The decomposition of the continuum spin $\boldsymbol{W}$ is given as follows:

$$\boldsymbol{W} = \boldsymbol{\Omega} + \boldsymbol{W}^{\mathrm{p}}, \tag{26.2}$$

where $\boldsymbol{W}^{\mathrm{p}}$ denotes the plastic spin and $\boldsymbol{\Omega}$ is the spin of substructures. The constitutive equation of elasticity is expressed as follows:

$$\overset{\circ}{\boldsymbol{\sigma}} = \dot{\boldsymbol{\sigma}} - \boldsymbol{\Omega}\boldsymbol{\sigma} + \boldsymbol{\sigma}\boldsymbol{\Omega} = \boldsymbol{C} : \boldsymbol{D}^{\mathrm{e}}, \tag{26.3}$$

where $\boldsymbol{\sigma}$ and $\overset{\circ}{\boldsymbol{\sigma}}$ are the Cauchy stress and its objective rate, respectively, $\boldsymbol{\Omega}$ is the spin tensor; and $\boldsymbol{C}$ is the elasticity modulus tensor. The initial yield criterion is expressed by the following equation:

$$f = \phi_0(\boldsymbol{\sigma}) - Y = \overline{\sigma}(\boldsymbol{\sigma}) - Y = 0, \tag{26.4}$$

where Y is the initial yield stress and $\overline{\sigma}$ is the effective stress. To describe the Bauschinger effect, as well as the evolutionary change of anisotropy, the subsequent yielding is expressed by the following equation:

$$f = \phi(\boldsymbol{\sigma} - \boldsymbol{\alpha}, \overline{\varepsilon}) - Y = \overline{\sigma}(\widetilde{\boldsymbol{\sigma}}, \overline{\varepsilon}) - Y = 0, \qquad \widetilde{\boldsymbol{\sigma}} = \boldsymbol{\sigma} - \boldsymbol{\alpha}, \tag{26.5}$$

where $\boldsymbol{\alpha}$ denotes the backstress. Based on the following definitions of the effective plastic strain and its rate

$$\overline{\sigma}\dot{\overline{\varepsilon}} = \widetilde{\boldsymbol{\sigma}} : \boldsymbol{D}^{\mathrm{p}}, \qquad \overline{\varepsilon} = \int \dot{\overline{\varepsilon}} \mathrm{d}t, \tag{26.6}$$

the associated flow rule is written as follows:

$$\boldsymbol{D}^{\mathrm{p}} = \frac{\partial f}{\partial \widetilde{\boldsymbol{\sigma}}} \dot{\lambda} = \frac{\partial \phi}{\partial \widetilde{\boldsymbol{\sigma}}} \dot{\lambda} \tag{26.7}$$

where $\dot{\lambda} = \dot{\overline{\varepsilon}}$.

Most kinematic hardening models assume the following form of the evolution equation of the back stress:

$$\overset{\circ}{\boldsymbol{\alpha}} = \left\{ \frac{A}{Y}(\boldsymbol{\sigma} - \boldsymbol{\alpha}) - \boldsymbol{x} \right\} \dot{\overline{\varepsilon}} = \left(\frac{A}{Y}\widetilde{\boldsymbol{\sigma}} - \boldsymbol{x} \right) \dot{\overline{\varepsilon}}, \tag{26.8}$$

Here $(\overset{\circ}{\ldots})$ denotes the objective rate. For example, in the linear kinematic hardening model:

$$\overset{\circ}{\boldsymbol{\alpha}} = \frac{H'_{LK}}{Y}(\boldsymbol{\sigma} - \boldsymbol{\alpha})\dot{\overline{\varepsilon}} = \frac{H'_{LK}}{Y}\widetilde{\boldsymbol{\sigma}}\dot{\overline{\varepsilon}}, \qquad A = H'_{LK}, \boldsymbol{x} = \boldsymbol{0} \tag{26.9}$$

In the Armstrong-Frederick model (Armstrong and Frederick 1966):

$$\overset{\circ}{\boldsymbol{\alpha}} = \left\{ \frac{\gamma_1}{Y}(\boldsymbol{\sigma} - \boldsymbol{\alpha}) - \gamma_2 \boldsymbol{\alpha} \right\} \dot{\bar{\varepsilon}} = \left(\frac{\gamma_1}{Y} \widetilde{\boldsymbol{\sigma}} - \gamma_2 \boldsymbol{\alpha} \right) \dot{\bar{\varepsilon}}, \qquad A = \gamma_1, \boldsymbol{x} = \gamma_2 \boldsymbol{\alpha} \tag{26.10}$$

The Y-U kinematic hardening law has the same form (for details, see the following section). The constitutive equation is given by the following form:

$$\overset{\circ}{\boldsymbol{\sigma}} = \boldsymbol{C}^{\mathrm{ep}} : \boldsymbol{D}, \tag{26.11}$$

$$\boldsymbol{C}^{\mathrm{ep}} = \begin{cases} \boldsymbol{C} & \text{if } \dot{\lambda} = 0 \\ \boldsymbol{C} - \dfrac{\boldsymbol{C} : \dfrac{\partial \phi}{\partial \widetilde{\boldsymbol{\sigma}}} \otimes \boldsymbol{C} : \dfrac{\partial \phi}{\partial \widetilde{\boldsymbol{\sigma}}}}{\dfrac{\partial \phi}{\partial \widetilde{\boldsymbol{\sigma}}} : \boldsymbol{C} : \dfrac{\partial \phi}{\partial \widetilde{\boldsymbol{\sigma}}} + H' - \dfrac{\partial \phi}{\partial \bar{\varepsilon}}} & \text{if } \dot{\lambda} > 0 \end{cases} \tag{26.12}$$

where

$$H' = A - \frac{\partial \phi}{\partial \widetilde{\boldsymbol{\sigma}}} : \boldsymbol{x} \tag{26.13}$$

26.3 Cyclic Plasticity Model to Describe the Bauschinger Effect and Workhardening Stagnation: Yoshida-Uemori Model

The Y-U model was constructed within the framework of two-surface modeling (Krieg 1975), wherein the yield surface moves kinematically within a bounding surface, as schematically illustrated in Fig. 26.2. To describe anisotropic hardening (i.e., expansion of the surface with shape change) and also kinematic hardening, the bounding surface F is expressed by the equation:

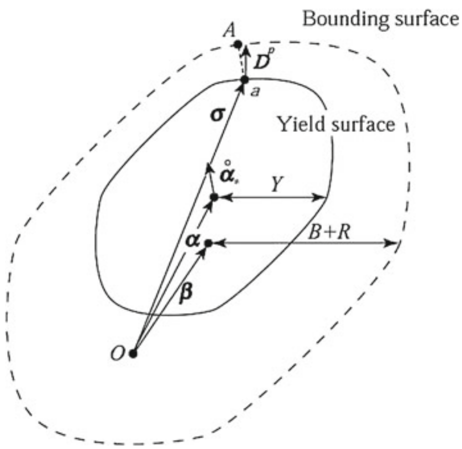

Fig. 26.2 Schematic illustration of the Yoshida-Uemori two-surface model

$$F = \phi(\boldsymbol{\sigma} - \boldsymbol{\beta}, \bar{\varepsilon}) - (B + R) = 0, \tag{26.14}$$

where $\boldsymbol{\beta}$ denotes the center of the bounding surface, and B and R are the initial size of the surface and its workhardening component, respectively. To include the description of anisotropic hardening in the model, it is assumed that the shapes of both the yield and bounding surfaces vary simultaneously.

The kinematic hardening of the yield surface describes the transient Bauschinger deformation, which is characterized by early re-yielding and subsequent rapid change in workhardening rate. The relative kinematic motion of the yield surface with respect to the bounding surface is expressed by the following equation:

$$\boldsymbol{\alpha}_* = \boldsymbol{\sigma} - \boldsymbol{\beta} \tag{26.15}$$

The evolution of $\boldsymbol{\alpha}_*$ is given by the following equation:

$$\overset{\circ}{\boldsymbol{\alpha}}_* = C\left\{\left(\frac{a}{Y}\right)(\boldsymbol{\sigma} - \boldsymbol{\alpha}) - \sqrt{\frac{a}{\bar{\boldsymbol{\alpha}}_*}}\right\}\dot{\bar{\varepsilon}} = \left\{\left(\frac{Ca}{Y}\right)\tilde{\boldsymbol{\sigma}} - C\sqrt{\frac{a}{\bar{\boldsymbol{\alpha}}_*}}\right\}\dot{\bar{\varepsilon}}, \tag{26.16}$$

$$\bar{\alpha}_* = \phi(\boldsymbol{\alpha}_*), \qquad a = B + R - Y \tag{26.17}$$

An Armstrong-Frederick-type evolution equation is used to express the kinematic hardening of $\boldsymbol{\beta}$

$$\overset{\circ}{\boldsymbol{\beta}}_* = k\left\{\left(\frac{b}{Y}\right)(\boldsymbol{\sigma} - \boldsymbol{\alpha}) - \boldsymbol{\beta}\right\}\dot{\bar{\varepsilon}} = \left(\frac{kb}{Y}\tilde{\boldsymbol{\sigma}} - k\boldsymbol{\beta}\right)\dot{\bar{\varepsilon}} \tag{26.18}$$

Thus, in Eq. (26.8),

$$A = Ca + kb, \qquad \boldsymbol{x} = C\sqrt{\frac{a}{\bar{\alpha}_*}}\boldsymbol{\alpha} - \left(C\sqrt{\frac{a}{\bar{\alpha}_*}} - k\right)\boldsymbol{\beta} \tag{26.19}$$

and in Eq. (26.13).
With respect to the expansion of the bounding surface, i.e., the evolution of R, in the first version of the Y-U model (Yoshida and Uemori 2002, 2003), the following equation based on the Voce hardening law (Voce 1948) was proposed:

$$R = R_{\mathrm{Voce}} = R_{\mathrm{sat}}\{1 - \exp(-k\bar{\varepsilon})\}, \tag{26.20}$$

written as

$$\dot{R} = \dot{R}_{\mathrm{Voce}} = k(R_{\mathrm{sat}} - R_{\mathrm{Voce}})\dot{\bar{\varepsilon}} \tag{26.21}$$

However, it is not necessary to use the Voce-type formulation. For example, based on the Swift law (Swift 1952):

$$R = R_{\mathrm{Swift}} = K\{(\varepsilon_0 + \bar{\varepsilon})^n - \varepsilon_0^n\}, \tag{26.22}$$

the following evolution equation can be obtained

$$\dot{R} = \dot{R}_{\mathrm{Swift}} = nK^{1/n}(R_{\mathrm{Swift}} + K\varepsilon_0^n)^{(n-1)/n}\dot{\bar{\varepsilon}} \tag{26.23}$$

Furthermore, a combination of the above two hardening laws, Eqs. (26.22) and (26.23), is also possible and can be expressed as follows:

$$\dot{R} = \omega\dot{R}_{\mathrm{Swift}} + (1-\omega)\dot{R}_{\mathrm{Voce}}, \qquad 0 \le \omega \le 1 \tag{26.24}$$

where ω is a weighting coefficient. This model has high flexibility in describing various levels of workhardening at large strain levels.

One of the features of the Yoshida-Uemori model is that it is able to describe the *workhardening stagnation* that appears in a reverse stress-strain curve for a certain range of reverse deformation (see Hasegawa and Yakou 1975; Christodoulou et al. 1986). This phenomenon is closely related to the strain-range and mean-strain dependency of cyclic hardening. Specifically, the larger the cyclic strain range is, the larger the saturated stress amplitudes are. This dependency is expressed by the stagnation of the expansion of the bounding surface for a certain range of reverse deformation. The states of hardening ($\dot{R} > 0$) and non-hardening ($\dot{R} = 0$) of the bounding surface are determined for a so-called non-IH (isotropic hardening) surface, g_σ, defined in the stress space as follows and schematically illustrated in Fig. 26.3a, b:

$$g_\sigma = \phi(\boldsymbol{\sigma} - \boldsymbol{q}, r) - r = 0, \tag{26.25}$$

where $\boldsymbol{q}$ and r denote the center and size of the non-IH surface, respectively. It is assumed that the center of the bounding surface $\boldsymbol{q}$ exists either on or inside of the surface g_σ. The expansion of the bounding surface takes place only when the center point of the bounding surface, $\boldsymbol{q}$, lies on the surface g_σ (see Fig. 26.3b), i.e., when

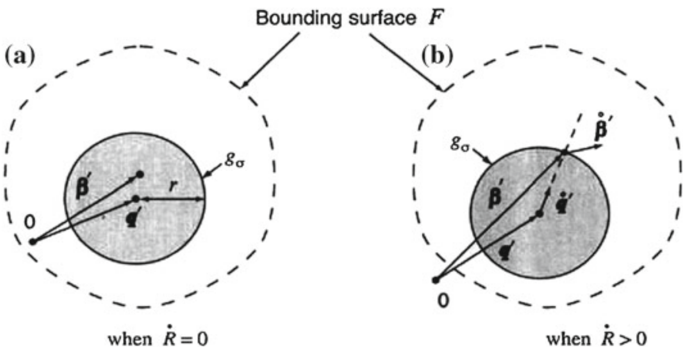

Fig. 26.3 Schematic illustration of the non-IH surface defined in the stress space, when expansion of the bounding surface **a** stops, and **b** takes place (Yoshida and Uemori 2003)

$$\dot{R} > 0 : g_\sigma(\boldsymbol{\beta} - \boldsymbol{q}, r) = \phi(\boldsymbol{\beta} - \boldsymbol{q}, r) - r = 0 \tag{26.26}$$

and

$$\dot{R} = 0 : \Gamma = \frac{\partial g_\sigma(\boldsymbol{\beta} - \boldsymbol{q}, r)}{\partial \boldsymbol{\beta}} : \overset{\circ}{\boldsymbol{\beta}} > 0 \tag{26.27}$$

otherwise. In an analysis of some experimental data, the plastic strain region of workhardening stagnation was found to increase with the accumulated plastic strain. To describe this phenomenon, it was assumed that the surface g_σ moves kinematically as it expands. The governing equations of the kinematic motion and expansion of the surface are given by Eqs. (26.28) and (26.29), respectively.

$$\overset{\circ}{\boldsymbol{q}} = \frac{(1-h)\Gamma}{r}(\boldsymbol{\beta} - \boldsymbol{q}), \tag{26.28}$$

$$\dot{r} = h\Gamma \tag{26.29}$$

Here, h is a parameter that controls the strength of the workhardening stagnation characteristic. A larger value of h corresponds to a larger strain region within which workhardening stagnation occurs, and as a result, a larger value of h leads to weaker cyclic hardening of a material. We may assume that the shape of the surface g_σ, is fixed $\phi = \phi_0$, or even $\phi =$ von Mises type, throughout the deformation, because the shape of g_σ has not been measured experimentally yet, and its effect on the stress-strain calculation would be rather minor.

Models of workhardening stagnation were recently reviewed by Ohno (2015). It should be noted that Ohno's model of non-isotropic-hardening, where the non-hardening region is expressed in the plastic strain space, is identical to the infinitesimal-strain Yoshida-Uemori model when assuming a linear kinematic hardening of the bounding surface.

In the proposed model, the size of the yield surface is held constant. However, if we carefully observe the stress-strain response during unloading after plastic deformation, we find that the stress-strain curve is no longer linear but rather is slightly curved due to very early re-yielding and the Bauschinger effect. To describe this phenomenon, in the model, the following equation for *plastic-strain-dependent Young's modulus* is introduced (Yoshida et al. 2002):

$$E = E_0 - (E_0 - E_\alpha)\{1 - \exp(-\xi\bar{\varepsilon})\}, \tag{26.30}$$

where E_0 and E_α are Young's modulus for virgin and infinitely large pre-strained materials, respectively, and ξ is a material constant.

Figure 26.4 shows stress-strain responses of 780 MPa high strength steel sheets under cyclic straining and uniaxial tension, calculated by the Y-U model, together with the corresponding experimental results.

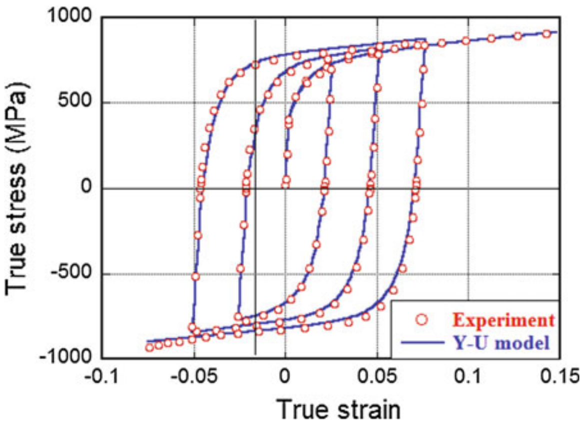

Fig. 26.4 Stress-strain curves for 780 MPa HSS sheet calculated with the Y-U model and the corresponding experimental data

26.4 Description of Evolution of Anisotropy

The evolution of anisotropy is expressed by the anisotropic hardening of the yield surface, as follows (refer to Yoshida et al. 2015):

$$\phi(\widetilde{\boldsymbol{\sigma}}, \bar{\varepsilon}) = \mu(\bar{\varepsilon})\phi_A(\widetilde{\boldsymbol{\sigma}}) + (1 - \mu(\bar{\varepsilon}))\phi_B(\widetilde{\boldsymbol{\sigma}}) \quad \text{for} \quad \bar{\varepsilon}_A \le \bar{\varepsilon} \le \bar{\varepsilon}_B \tag{26.31}$$

Here, $\phi_A(\widetilde{\boldsymbol{\sigma}})$ and $\phi_B(\widetilde{\boldsymbol{\sigma}})$ are two different yield functions defined at the effective plastic strains $\bar{\varepsilon}_A$ and $\bar{\varepsilon}_B$, respectively, i.e., $\phi_A(\widetilde{\boldsymbol{\sigma}}) = \phi(\widetilde{\boldsymbol{\sigma}}, \bar{\varepsilon}_A)$ and $\phi_B(\widetilde{\boldsymbol{\sigma}}) = \phi(\widetilde{\boldsymbol{\sigma}}, \bar{\varepsilon}_B)$, and $\mu(\bar{\varepsilon})$ an interpolation function of the effective plastic strain, where

$$1 = \mu(\bar{\varepsilon}_A) \ge \mu(\bar{\varepsilon}) \ge \mu(\bar{\varepsilon}_B) = 0 \tag{26.32}$$

Note that the types of these two yield functions, $\phi_A(\widetilde{\boldsymbol{\sigma}})$ and $\phi_B(\widetilde{\boldsymbol{\sigma}})$, do not need to be the same. An advantage of this modeling framework is that, if the two yield functions $\phi_A(\widetilde{\boldsymbol{\sigma}})$ and $\phi_B(\widetilde{\boldsymbol{\sigma}})$ are convex, $\phi(\widetilde{\boldsymbol{\sigma}}, \bar{\varepsilon})$ always satisfies the convexity. The derivatives are expressed as follows:

$$\frac{\partial \phi}{\partial \widetilde{\boldsymbol{\sigma}}} = \mu(\bar{\varepsilon})\frac{\partial \phi_A(\widetilde{\boldsymbol{\sigma}})}{\partial \widetilde{\boldsymbol{\sigma}}} + (1 - \mu(\bar{\varepsilon}))\frac{\partial \phi_B(\widetilde{\boldsymbol{\sigma}})}{\partial \widetilde{\boldsymbol{\sigma}}}, \qquad \frac{\partial \phi}{\partial \bar{\varepsilon}} = (\phi_A(\widetilde{\boldsymbol{\sigma}}) - \phi_B(\widetilde{\boldsymbol{\sigma}}))\frac{\partial \mu(\bar{\varepsilon})}{\partial \bar{\varepsilon}} \tag{26.33}$$

Several linear and nonlinear functions can be used for the interpolation function $\mu(\bar{\varepsilon})$. Assuming that $\bar{\varepsilon}_A = 0$ (at initial yielding) and $\bar{\varepsilon}_A = \infty$ (at infinitely large strain) and that $\phi_A(\widetilde{\boldsymbol{\sigma}}) = \phi_0(\widetilde{\boldsymbol{\sigma}}) = \phi_0(\boldsymbol{\sigma})$ and $\phi_B(\widetilde{\boldsymbol{\sigma}}) = \phi_\infty(\widetilde{\boldsymbol{\sigma}})$, Eq. (26.31) reduces to the following

$$\phi(\widetilde{\boldsymbol{\sigma}}, \bar{\varepsilon}) = \mu(\bar{\varepsilon})\phi_0(\widetilde{\boldsymbol{\sigma}}) + (1 - \mu(\bar{\varepsilon}))\phi_\infty(\widetilde{\boldsymbol{\sigma}}) \quad 0 \le \bar{\varepsilon} \le 0 \tag{26.34}$$

Some examples of forms of interpolation functions are as follows:

$$\mu(\bar{\varepsilon}) = \exp(-\lambda\bar{\varepsilon}), \tag{26.35}$$

$$\mu(\bar{\varepsilon}) = a\exp(-\lambda_1\bar{\varepsilon}) + (1-a)\exp(-\lambda_2\bar{\varepsilon}), \tag{26.36}$$

where λ, a, λ_1 and λ_2 are material constants.

If we have M sets of experimental data ($\sigma_0, \sigma_{45}, \sigma_{90}, \sigma_b, r_0, r_{45}, r_{90}$, etc.) for material parameter identification corresponding to M discrete plastic strain points, $\bar{\varepsilon}_1(=0), \bar{\varepsilon}_2, \ldots, \bar{\varepsilon}_i, \bar{\varepsilon}_{i+1}, \ldots, \bar{\varepsilon}_M$, we can determine M sets of yield functions $\phi_1(\tilde{\boldsymbol{\sigma}}), \phi_2(\tilde{\boldsymbol{\sigma}}), \ldots, \phi_i(\tilde{\boldsymbol{\sigma}}), \phi_{i+1}(\tilde{\boldsymbol{\sigma}}), \ldots, \phi_M(\tilde{\boldsymbol{\sigma}})$. Using an interpolation function $\mu(\bar{\varepsilon})$, the yield function $\phi(\tilde{\boldsymbol{\sigma}}, \bar{\varepsilon})$ can be defined by the following equation:

$$\phi(\tilde{\boldsymbol{\sigma}}, \bar{\varepsilon}) = \mu(\bar{\varepsilon})\phi_i(\tilde{\boldsymbol{\sigma}}) + (1-\mu(\bar{\varepsilon}))\phi_{i+1}(\tilde{\boldsymbol{\sigma}}) \qquad \text{for} \qquad \bar{\varepsilon}_i \le \bar{\varepsilon} \le \bar{\varepsilon}_{i+1} \tag{26.37}$$

The following nonlinear equation is proposed for use as the interpolation function:

$$\mu(\bar{\varepsilon}) = 1 - \left(\frac{\bar{\varepsilon} - \bar{\varepsilon}_i}{\bar{\varepsilon}_{i+1} - \bar{\varepsilon}_1}\right)^{p_i} \qquad \bar{\varepsilon}_i \le \bar{\varepsilon} \le \bar{\varepsilon}_{i+1}, \tag{26.38}$$

where $p_i (i = 1, 2, \ldots, M-1)$ are material constants.

Among the various types of anisotropic yield functions available, stress polynomial-type models (e.g., Hill 1948; Gotoh 1977; Soare et al. 2008; Yoshida et al. 2013) are suitable for use in modeling anisotropy evolution. A polynomial-type yield criterion is given by the following equation:

$$f = \phi^{(m)}(\boldsymbol{\sigma}) - Y^m = \bar{\sigma}^m - Y^m = 0, \tag{26.39}$$

where $\phi^{(m)}(\boldsymbol{\sigma})$ denotes the mth order stress polynomial-type yield function. For example, when $m = 6$ (Yoshida et al. 2013) under plane stress condition,

$$\begin{aligned}\phi^{(6)} = {} & C_1\sigma_x^6 - 3C_2\sigma_x^5\sigma_y + 6C_3\sigma_x^4\sigma_y^2 - 7C_4\sigma_x^3\sigma_y^3 + 6C_3\sigma_x^2\sigma_y^4 - 3C_6\sigma_x\sigma_y^5 \\ & + C_7\sigma_y^6 + 9(C_8\sigma_x^4 - 2C_9\sigma_x^3\sigma_y + 3C_{10}\sigma_x^2\sigma_y^2 - 2C_{11}\sigma_x\sigma_y^3 + 2C_{12}\sigma_y^4)\tau_{xy}^2 \\ & + 27(C_{13}\sigma_x^2 - C_{14}\sigma_x\sigma_y + C_{15}\sigma_y^2)\tau_{xy}^4 + 27C_{16}\tau_{xy}^6\end{aligned} \tag{26.40}$$

In the same manner as Eq. (26.31), when the following equation is assumed

$$\phi^{(m)}(\tilde{\boldsymbol{\sigma}}, \bar{\varepsilon}) = \mu(\bar{\varepsilon})\phi_A^{(m)}(\tilde{\boldsymbol{\sigma}}) + (1-\mu(\bar{\varepsilon}))\phi_B^{(m)}(\tilde{\boldsymbol{\sigma}}), \tag{26.41}$$

it reduces to an interpolation for material parameters C_k, $k = 1, 2, \ldots, N$, as follows

$$C_k = \mu(\bar{\varepsilon})C_{k(A)} + (1-\mu(\bar{\varepsilon}))C_{k(B)} \tag{26.42}$$

Here, $C_{k(A)}$ and $C_{k(B)}$ are material parameters determined at the effective plastic strains, $\bar{\varepsilon}_A$ and $\bar{\varepsilon}_B$, respectively. Assuming that $\bar{\varepsilon}_A = 0$ (at initial yielding) and $\bar{\varepsilon}_B = \infty$ (at infinitely large strain) and that $C_{k(A)} = C_{k(0)}$ and $C_{k(B)} = C_{k(\infty)}$, Eq. (26.42) reduces to the following:

$$C_k = \mu(\bar{\varepsilon})C_{k(0)} + (1 - \mu(\bar{\varepsilon}))C_{k(\infty)}, \qquad 0 \le \bar{\varepsilon} \le \infty \tag{26.43}$$

In discretization form:

$$C_k = \mu(\bar{\varepsilon})C_{k(i)} + (1 - \mu(\bar{\varepsilon}))C_{k(i+1)}, \qquad i = 1, 2, \ldots, M - 1 \tag{26.44}$$

To validate the model, calculated stress-strain responses were compared with the corresponding experimental data for AA6022-T43 aluminum sheet (Stoughton and Yoon 2009). As for the yield function, sixth-order polynomial model is employed. One of advantages of this model is that, flow stresses $\sigma_0, \sigma_{45}, \sigma_{90}, \sigma_b$ and r-values r_0, r_{45}, r_{90} are calculated by using the material parameters $C_1 \sim C_{16}$ explicitly. Thus the material parameters are easily identified.

$$\sigma_{90} = \left(\frac{C_1}{C_7}\right)^{\frac{1}{6}} \sigma_0, \quad \sigma_{45} = \left(\frac{C_1}{S + 9T + 27U + 27C_{16}}\right)^{\frac{1}{6}} \sigma_0, \quad \sigma_b = \left(\frac{C_1}{S}\right)^{\frac{1}{6}} \sigma_0, \tag{26.45}$$

$$r_0 = \frac{C_2}{2C_1 - C_2}, \quad r_{45} = \frac{-S - 3T + 9U + C_{16}}{2S + 12T + 18U}, \quad r_{90} = \frac{C_6}{2C_7 + C_6} \tag{26.46}$$

$$\begin{aligned} S &= C_1 - 3C_2 + 6C_3 - 7C_4 + 6C_5 - 3C_6 + C_7, \\ T &= C_8 - 2C_9 + 3C_{10} - 2C_{11} + C_{12}, \\ U &= C_{13} - C_{14} + 3C_{15} \end{aligned}$$

On AA6022-T43 aluminum sheet, r-value planar anisotropy remains fixed throughout the plastic deformation. In this calculation the kinematic hardening was excluded since in monotonic loading the stress-strain calculation is not affected by the kinematic hardening. The results of flow stresses, $\sigma_0, \sigma_{45}, \sigma_{90}, \sigma_b$ calculated using Eqs. (26.44) and (26.38), with $M = 3$, are compared to the experimental data, as shown in Fig. 26.5. Here, three discrete plastic strain points, $\bar{\varepsilon} = 0, 0.1$ and 0.5 are selected to define $\phi_1(\boldsymbol{\sigma})$, $\phi_2(\boldsymbol{\sigma})$ and $\phi_3(\boldsymbol{\sigma})$. The calculated results agree well overall with the experimental results for the stresses.

The model was also validated by comparing the calculated results of stress-strain responses with experimental data on r-value and stress-directionality changes in an aluminum sheet (Hu 2007) and a stainless steel sheet (Stoughton and Yoon 2009), as well as the variation of the yield surface of an aluminum sheet (Yanaga et al. 2014). Furthermore, anisotropic cyclic behavior was examined by performing experiments of uniaxial tension and cyclic straining in three sheet directions on a 780 MPa advanced high-strength steel sheet. For details of the results, refer to Yoshida et al. (2015).

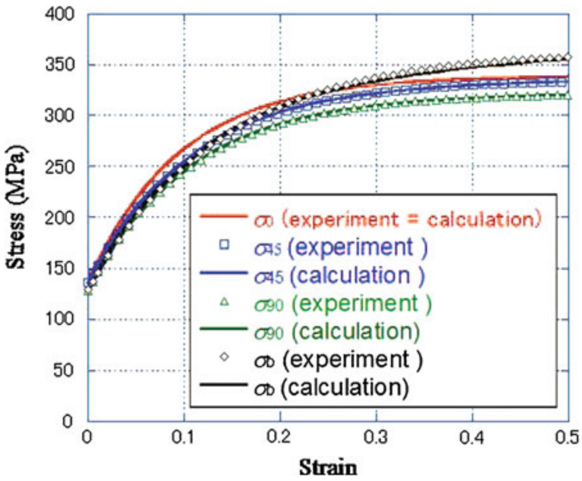

Fig. 26.5 Flow stresses of AA6022-T43 aluminum sheet predicted using the anisotropy evolution model

26.5 Concluding Remarks

The present paper describes a framework for the constitutive modeling of large-strain cyclic plasticity that describes the evolution of anisotropy and the Bauschinger effect of sheet metals based on the Y-U kinematic hardening model. The Y-U model predicts the springback much more accurately than the classical isotropic hardening model (e.g., refer to Yoshida and Uemori 2002; Eggertsen and Mattiasson 2009, 2010; Ghaei et al. 2010; Wagoner et al. 2013; Huh et al. 2011). It has gained popularity in the sheet metal forming industry because it has already been implemented into several FE commercial codes (e.g., PAM-STAMP, LS-DYNA, StamPack) and is widely used for springback simulation. The highlights of this modeling are summarized as follows.

- The Y-U model is highly capable of describing various cyclic plasticity characteristics such as the Bauschinger effect, the workhardening stagnation, strain-range-dependent cyclic workhardening, and the degradation of unloading stress-strain slope with increasing plastic strain. Furthermore, any type of anisotropic yield function can be used.
- It requires a limited number of material parameters (seven or eight plasticity parameters and three elasticity parameters including Young's modulus). The scheme for material parameter identification and testing have been clearly presented, see Yoshida and Uemori (2002).
- The evolution of the anisotropy can be described by incorporating the proposed anisotropic hardening model in the Y-U model. In this modeling framework a set of kinematic hardening parameters can be identified experimentally independent of anisotropic hardening parameters, and their values remain fixed throughout the plastic deformation
- An anisotropic yield function that varies continuously with the plastic strain is defined by a nonlinear interpolation function of the effective plastic strain using a

limited number of yield functions determined at a few discrete points of the plastic strain. In this modeling framework, it is possible to use any type of yield function, and the convexity of the yield surface is always guaranteed.

- This approach, which requires only one interpolation equation, offers a great advantage over other approaches in that it involves fewer material parameters.

Acknowledgments The authors are sincerely grateful to Professor Nobutada Ohno of Nagoya University for fruitful discussions on cyclic plasticity modeling for so long years.

References

An YG, Vegter H, Melzer S, Triguero PR (2013) Evolution of the plastic anisotropy with straining and its implication on formability for sheet metals. J Mater Process Technol 213:1419–1425

Armstrong PJ, Frederick CO (1966) A mathematical representation of the multiaxial bauschinger effect. Technical Report GEGB report RD/B/N731, Berkley Nuclear Laboratories

Banabic D, Aretz H, Comsa DS, Paraianu L (2005) An improved analytical description of orthotropy in metallic sheets. Int J Plast 21:493–512

Barlat F, Lian J (1989) Plastic behavior and stretchability of sheet metals. Part 1. a yield function for orthotropic sheets under plane-stress conditions. Int J Plast 5:51–66

Barlat F, Lege DJ, Brem JC (1991) A 6-component yield function for anisotropic materials. Int J Plast 7(7):693–712

Barlat F, Brem JC, Yoon JW, Chung K, Dick RE, Lege DJ, Pourgoghrat F, Choi SH, Chu E (2003) Plane stress yield function for aluminum alloy sheets—Part 1: theory. Int J Plast 19:1297–1319

Barlat F, Aretz H, Yoon JW, Karabin ME, Brem JC, Dick RE (2005) Linear transformation-based anisotropic yield functions. Int J Plast 21:1009–1039

Barlat F, Gracio JJ, Lee MJ, Rauch EF, Vincze G (2011) An alternative to kinematic hardening in classical plasticity. Int J Plast 27:1309–1327

Barlat F, Ha J, Gracio JJ, Lee MJ, Rauch EF, Vincze G (2013) Extension of homogeneous anisotropic hardening model to cross-loading with latent effects. Int J Plast 46:130–142

Barlat F, Vincze G, Gracio JJ, Lee MJ, Rauch EF, Tome CN (2014) Enhancements of homogeneous anisotropic hardening model and application to mild and dual-phase steels. Int J Plast 58:201–218

Bron F, Besson J (2004) A yield function for anisotropic materials, application to aluminum alloys. Int J Plast 20:937–963

Cazacu O, Barlat F (2001) Generalization of Drucker's yield criterion to orthotropy. Math Mech Solids 6:613–630

Cazacu O, Barlat F (2003) Application of the theory of representation to describe yielding of anisotropic aluminum alloys. Int J Eng Sci 41:1367–1385

Cazacu O, Barlat F (2004) A criterion for description of anisotropy and yield differential effects in pressure-insensitive metals. Int J Plast 20:2027–2045

Chaboche JL (2008) A review of some plasticity and viscoplasticity constitutive theories. Int J Plast 24:1642–1693

Chaboche JL, Rousselier G (1983) On the plastic and viscoplastic constitutive equations, Part I and II. Trans ASME J Press Vessel Technol 105:153–164

Christodoulou N, Woo OT, MacEwen SR (1986) EEffect of stress reversals on the work hardening behaviour of polycrystalline copper. Acta Metall 34:1553–1562

Comsa DS, Banabic D (2008) Plane-stress yield criterion for highly-anisotropic sheet metals. In: Hora P (ed) Proceedings of the 7th International conference and workshop on numerical simulation of 3D sheet metal forming processes (NUMISHEET 2008), pp 43–48

Dafalias YF, Popov EP (1976) Plastic internal variables formalism of cyclic plasticity. Trans ASME J Appl Mech 43:645–651
Desmorat R, Marull R (2011) Non quadratic Kelvin modes based plasticity criteria for anisotropic materials. Int J Plast 27:328–351
Eggertsen PA, Mattiasson K (2009) On the modelling of the bending-unbending behaviour for accurate springback predictions. Int J Mech Sci 51:547–563
Eggertsen PA, Mattiasson K (2010) On constitutive modeling of springback analysis. Int J Mech Sci 52:804–818
Feigenbaum HP, Dafalias YF (2007) Directional distortional hardening in metal plasticity with thermodynamics. Int J Solids Struct 44:7526–7542
Francois M (2001) A plasticity model with yield surface distortion for non-proportional loading. Int J Plast 17:703–717
Geng LM, Wagoner RH (2002) Role of plastic anisotropy and its evolution on spring-back. Int J Mech Sci 44:123–148
Ghaei A, Green DE, Taherizadeh A (2010) Semi-implicit numerical integration of Yoshida-Uemori two-surface plasticity model. Int J Mech Sci 52:531–540
Gotoh M (1977) Theory of plastic anisotropy based on a yield function of 4th-order (plane stress state)-1. Int J Mech Sci 19:505–512
Haddadi H, Bouvier S, Banu M, Maier C, Teodosiu C (2006) Towards an accurate description of the anisotropic behavior of sheet metals under large plastic deformation: modelling, numerical analysis and identification. Int J Plast 22:2226–2271
Hasegawa T, Yakou T (1975) Deformation behaviour and dislocation structures upon stress reversal in polycrystalline aluminium. Mater Sci Eng 20:267–276
Hill R (1948) A theory of the yielding and plastic flow of anisotropic metals. Proc R Soc Lond A 193:281–297
Hill R (1979) Theoretical plasticity of textured aggregates. Math Proc Cambridge Philos Soc 85:179–191
Hill R (1990) Constitutive modeling of orthotropic plasticity in sheet metals. J Mech Phys Solids 38:405–417
Hu WL (2005) An orthotropic yield criterion in a 3-D general stress state. Int J Plast 21:1771–1796
Hu WL (2007) Constitutive modeling of orthotropic sheet metals by presenting hardening-induced anisotropy. Int J Plast 23:620–639
Huh H, Chung K, Han SS, Chung WJ (eds) (2011) NUMISHEET 2011, Part C: Benchmark problems and results, BM4—Pre-strain effect on spring-back of 2-D draw bending. The Korean Society for Technology of Plasticity, KAIST Press, Daejeon
Karafillis AP, Boyce MC (1993) A general anisotropic yield criterion using bounds and a transformation weighting tensor. J Mech Phys Solids 41:1859–1886
Krieg RD (1975) A practical two surface plasticity theory. Trans ASME J Appl Mech 42:641–646
Kurtyka T, Życzkowski M (1996) Evolution equations for distorsional plastic hardening. Int J Plast 12(2):191–213
Kuwabara T, Ikeda S, Kuroda K (1998) Measurement and analysis of differential work hardening in cold-rolled steel sheet under biaxial tension. J Mater Process Tech 80:517–523
Leacock AG (2006) A mathematical description of orthotropy in sheet metals. J Mech Phys Solids 54:425–444
MacDowell DL (1995) Stress state dependence of cyclic ratchetting behavior of two rail steels. Int J Plast 11:397–421
Mróz Z (1967) On the description of anisotropic workhardening. J Mech Phys Solids 15:163–175
Ohno N (1982) A constitutive model of cyclic plasticity with a non-hasrdening strain range. Trans ASME J Appl Mech 49:721–727
Ohno N (2015) Material models of cyclic plasticity with extended isotropic hardening: a review. Bull JSME: Mech Eng Rev 2(1):14-00425
Ohno N, Wang JD (1993) Nonlinear kinematic hardening rule with critical state of dynamic recovery. Part I: Formulation and basic features for ratchetting behavior. Int J Plast 9:375–390

Plunkett B, Cazacu O, Barlat F (2008) Orthotropic yield criteria for description of the anisotropy in tension and compression of sheet metals. Int J Plast 24:847–866
Safaei M, Lee MG, Zang S, Waele WD (2014) An evolutionary anisotropic model for sheet metals based on non-associated flow rule approach. Comput Mater Sci 81:15–29
Shiratori E, Ikegami K, Yoshida F (1979) Analysis of stress-strain relations by use of anisotropic hardening plastic potential. J Mech Phys Solids 27:213–229
Soare S, Yoon JW, Cazacu O (2008) On the use of homogeneous polynomials to develop anisotropic yield functions with applications to sheet forming. Int J Plast 24:915–944
Steglich D, Brocks W, Bohlen J, Barlat F (2011) Modelling direction-dependent hardening in magnesium sheet forming simulations. Int J Mater Forum 4:243–253
Stoughton TB, Yoon JW (2009) Anisotropic hardening and non-associated flow in proportional loading of sheet metals. Int J Plast 25:1777–1817
Swift HW (1952) Plastic instability under plane stress. J Mech Phys Solids 1:1–18
Taleb L (2013) About cyclic strain accumulation of the inelastic strain observed in metals subjected to cyclic stress control. Int J Plast 43:1–19
Tozawa Y (1978) Plastic deformation behavior under conditions of combined stress. In: Wang NM, Koistinen DP (eds) Mechanics of sheet metal forming. Plenum Press, New York, pp 81–110
Vegter H, van den Boogaard AH (2006) A plane stress yield function for anisotropic sheet material by interpolation of biaxial stress states. Int J Plast 22:557–580
Voce E (1948) The relationship between stress and strain for homogeneous deformation. J Inst Metals 74:537–562
Voyiadjis GZ, Foroozesh M (1990) Anisotropic distortional yield model. Trans ASME J Appl Mech 57:537–547
Wagoner RH, Lim H, Lee MG (2013) Advanced issue in springback. Int J Plast 45:3–20
Yanaga D, Takizawa H, Kuwabara T (2014) Formulation of differential work hardening of 6000 series aluminum alloy sheet and application to finite element analysis. Trans JSTP 55:55–61 (in Japanese)
Yoon JW, Lou Y, Yoon J, Glazoff MV (2014) Asymmetric yield function based on the stress invariants for pressure sensitive metals. Int J Plast 56:184–202
Yoshida F (2000) A constitutive model of cyclic plasticity. Int J Plast 16:359–380
Yoshida F, Uemori T (2002) A model of large-strain cyclic plasticity describing the bauschinger effect and workhardening stagnation. Int J Plast 18:661–686
Yoshida F, Uemori T (2003) A model of large-strain cyclic plasticity and its application to springback simulation. Int J Mech Sci 45:1687–1702
Yoshida F, Uemori T, Fujiwara K (2002) Elastic-plastic behavior of steel sheets under in-plane cyclic tension-compression at large strain. Int J Plast 18:633–659
Yoshida F, Hamasaki H, Uemori T (2008) A user-friendly 3D yield function to describe anisotropy of steel sheets. Int J Plast 45:119–139
Yoshida F, Hamasaki H, Uemori T (2013) A user-friendly 3D yield function to describe anisotropy of steel sheets. Int J Plast 45:119–139
Yoshida F, Hamasaki H, Uemori T (2015) Modeling of anisotropic hardening of sheet metals including description of the bauschinger effect. Int J Plast. doi:10.1016/j.ijplas.2015.02.004